

THE CHANGING LY α OPTICAL DEPTH IN THE RANGE $6 < Z < 9$ FROM MOSFIRE SPECTROSCOPY OF Y-DROPOUTS

TOMMASO TREU¹, KASPER B. SCHMIDT¹, MICHELE TRENTI², LARRY D. BRADLEY³, MASSIMO STIAVELLI³

¹ Department of Physics, University of California, Santa Barbara, CA, 93106-9530, USA

² Institute of Astronomy and Kavli Institute for Cosmology, University of Cambridge, Madingley Road, Cambridge, CB3 0HA, United Kingdom and

³ Space Telescope Science Institute, 3700 San Martin Drive, Baltimore, MD, 21218, USA

Draft version October 25, 2021

ABSTRACT

We present MOSFIRE spectroscopy of 13 candidate $z \sim 8$ galaxies selected as Y-dropouts as part of the BoRG pure parallel survey. We detect no significant Ly α emission (our median 1σ rest frame equivalent width sensitivity is in the range 2-16Å). Using the Bayesian framework derived in a previous paper, we perform a rigorous analysis of a statistical subsample of non-detections for ten Y-dropouts, including data from the literature, to study the cosmic evolution of the Ly α emission of Lyman Break Galaxies. We find that Ly α emission is suppressed at $z \sim 8$ by at least a factor of three with respect to $z \sim 6$ continuing the downward trend found by previous studies of z -dropouts at $z \sim 7$. This finding suggests a dramatic evolution in the conditions of the intergalactic or circumgalactic media in just 300 Myrs, consistent with the onset of reionization or changes in the physical conditions of the first generations of starforming regions.

Subject headings: galaxies: evolution — galaxies: high-redshift

1. INTRODUCTION

In the past few years our knowledge of the first galaxies has increased stupendously. Deep imaging surveys with the Hubble Space Telescope have pushed the frontier of Lyman Break galaxies (LBGs) beyond redshift $z \sim 10$ reaching into the epoch of cosmic reionization (e.g., Bouwens et al. 2010; Ellis et al. 2013; Robertson et al. 2013; Coe et al. 2013). The luminosity function of LBGs appears to evolve rapidly, with a decrease in the number density of observed galaxies, but with faint end slopes getting steeper (e.g., Bradley et al. 2012; Oesch et al. 2013). Similarly, narrow band surveys on large ground based telescopes have enabled searches for Ly α emission yielding many candidate galaxies at comparably high redshift (hereafter Ly α emitters, LAE). These studies indicate that the amount of ionizing photons from these galaxies is sufficient to keep the universe ionized, only if the luminosity function extends to very faint magnitudes and the ionizing fraction is high (Trenti et al. 2010; Lorenzoni et al. 2011).

Spectroscopic follow-up is key to further our understanding of the physics of the first galaxies, their interactions with the surrounding intergalactic medium, and their role in cosmic reionization. Even though spectroscopic follow-up of LBGs has been very successful out to $z \sim 6$, progress has been slower beyond this threshold. Several studies have shown that at $z \sim 7$ Ly α emission appears to be significantly reduced with respect to $z \sim 6$, consistent with a rapid rise in the fraction of neutral hydrogen in the immediate surroundings of these galaxies, possibly a smoking gun that we have reached the tail-end of cosmic reionization (Kashikawa et al. 2006; Fontana et al. 2010; Pentericci et al. 2011; Schenker et al. 2012; Ono et al. 2012; Treu et al. 2012).

Beyond $z \sim 7$, galaxies remain enshrouded in mystery, at least from a spectroscopic point of view. Confirmation of LBGs and even of some LAEs remain elusive (Lehnert et al. 2010; Bunker et al. 2013; Jiang et al. 2013; Capak et al. 2013). This stems in part from technological limitations as Ly α is redshifted into the near infrared where tra-

ditionally spectrographs did not have the sensitivity and multiplexing capabilities of their optical counterparts (see, e.g., Schenker et al. 2012; Treu et al. 2012).

We present here deep spectroscopic observations of a sample of 13 $z \sim 8$ galaxies selected as Y-band dropouts as part of the Brightest of Reionization Galaxies (hereafter BoRG Trenti et al. 2011; Bradley et al. 2012), using the new MOSFIRE (McLean et al. 2008; McLean et al. 2012) spectrograph on the Keck-I Telescope. The combination of BoRG and MOSFIRE is extremely powerful for the study of the $z \sim 8$ universe. The wide-area search of BoRG allows us to find the brightest candidate galaxies, which also happen to be clustered (Trenti et al. 2012) in the sky and are therefore ideal targets for the multiplexing capabilities of MOSFIRE.

No Ly α emission is detected down to median limiting fluxes of $0.4 - 0.6 \cdot 10^{-17}$ erg s⁻¹cm⁻² (5σ), whereas a few detections would have been expected if the distribution of Ly α emission had been the same as at $z \sim 6$ (Treu et al. 2012). We use the statistical framework developed by Treu et al. (2012) to perform a rigorous analysis of the non-detections, taking into account all the available information, and show that they imply a significant increase in the Ly α optical depth between $z \sim 6$ and $z \sim 8$.

All magnitudes are given in the AB system and a standard cosmology with $\Omega_m = 0.3$, $\Omega_\Lambda = 0.7$ and $h = 0.7$ is assumed.

2. OBSERVATIONS AND DATA REDUCTION

The spectroscopic targets were selected from BoRG as Y-band dropouts, i.e. $z \sim 8$ galaxy candidates, using *Hubble Space Telescope* (HST) data taken in the WFC3 bands F600LP/F606W, F098M, F125W, and F160W as described by Bradley et al. (2012) and Schmidt et al. (2013; in preparation). The spectroscopic sample presented here consists of 13 individual targets, from 3 of the 71 BoRG fields, namely BoRG_0951+3304, BoRG_1437+5043, and BoRG_1510+1115, selected to contain a large number of high-quality candidates. The primary statistical sample consists of 8 dropouts detected at high-significance ($>5\sigma$ in the primary detection band, plus all the color requirements) as

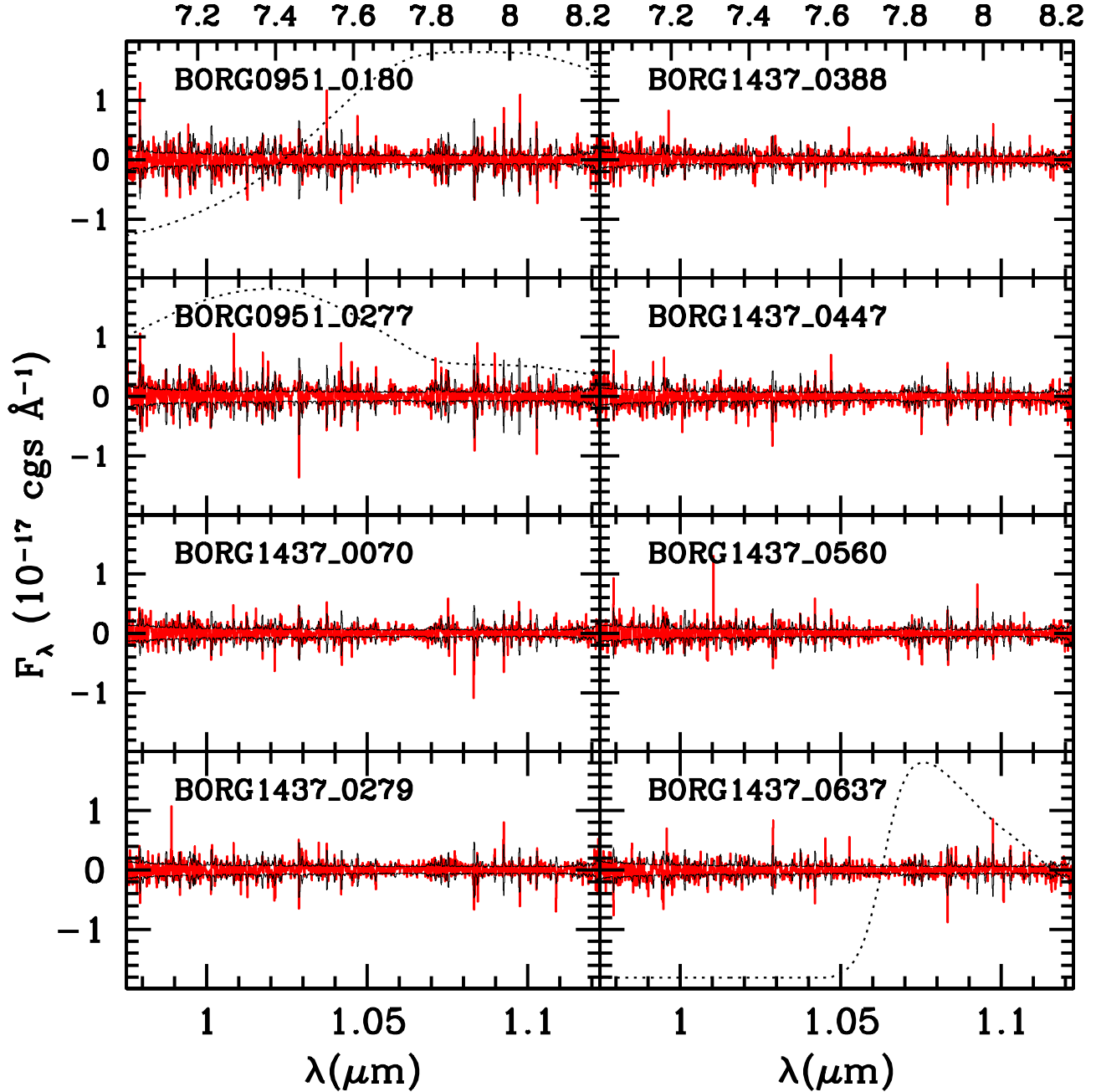


FIG. 1.— Mosaic of the reduced MOSFIRE spectra for targets with only Y band spectroscopic data. The red histogram shows the actual spectrum, while the black envelope shows the 1σ noise level. All spectra are consistent with pure noise. The top label shows the redshift coverage of the spectra for Ly α redshift. For all objects in the statistical sample (see discussion in text) the photometric redshift posterior distribution function is shown as the black dashed curve.

described by Schmidt et al. (2013; in preparation). Photometric redshifts for the sources in the primary sample are shown as dashed black curves in Figures 1 and 2. We took advantage of the multi-slit capabilities of MOSFIRE (McLean et al. 2012) to observe 5 marginal candidates. For completeness we present results from these 5 marginal objects but do not consider them in our statistical analysis.

The near-infrared spectroscopic data presented here were obtained with MOSFIRE on Keck-I during two nights (25-26 April 2013), in good weather with subarcsecond seeing and clear transparency. We used slit widths of $0''.7$ and a nodding amplitude of $1''.5$. BoRG_0951+3304, BoRG_1437+5043

were observed in the Y-band, whereas BoRG_1510+1115 was observed both in the Y and J bands. Table 1 summarizes exposure times. The spatial resolution is $0''.1799$ per pixel and the dispersion is 1.0855 and 1.3028 $\text{\AA}/\text{pixel}$ in Y and J respectively. The spectral coverage is shown in the Figures.

The data were reduced using the publicly available MOSFIRE data reduction pipeline (DRP¹). The output of the DRP are non-calibrated 2D spectra in units of electrons per second per pixel. From the 2D spectra, 1D spectra were extracted by using a 11 pixel-wide extraction aperture centered

¹ <http://code.google.com/p/mosfire/>

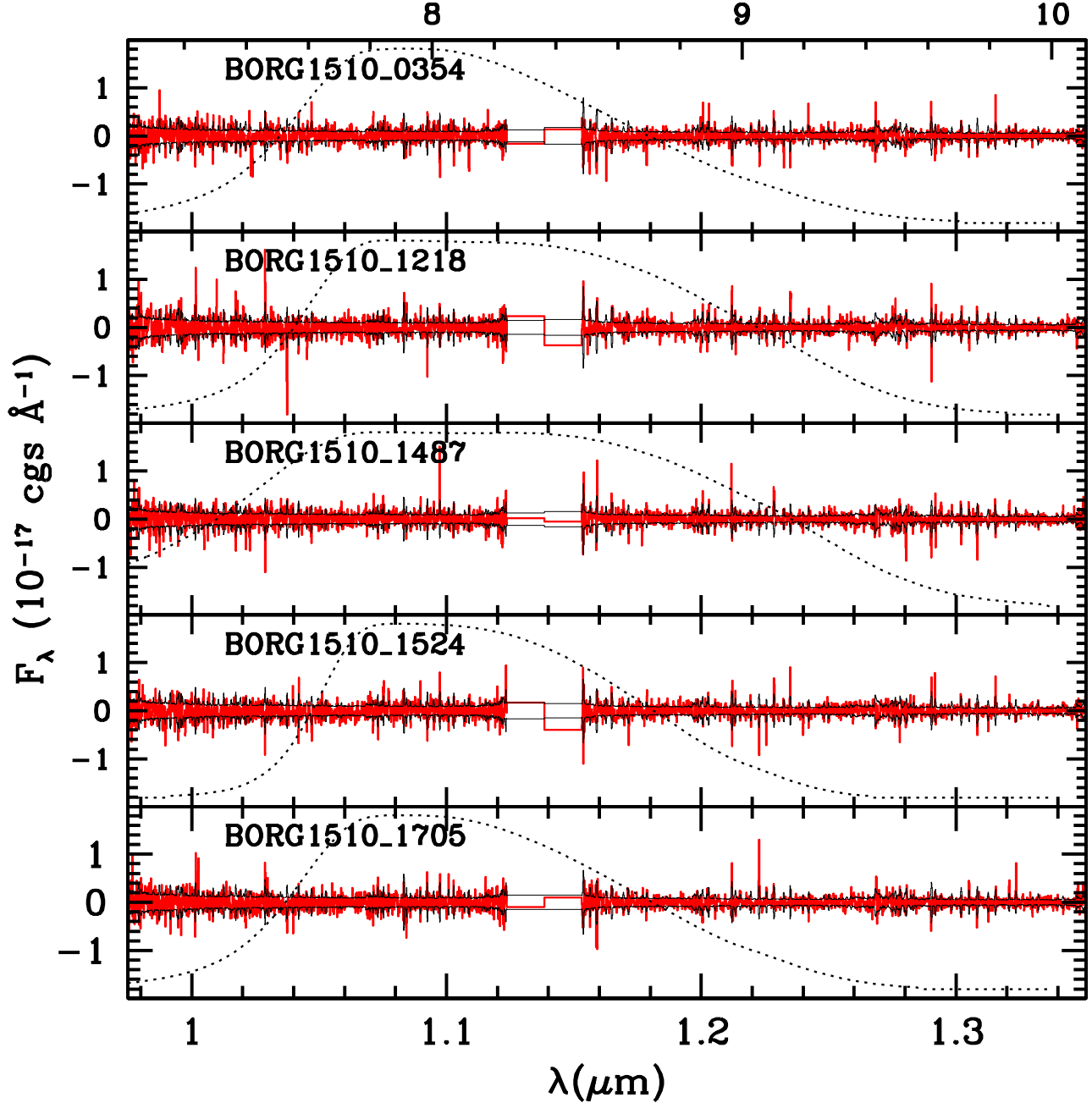


FIG. 2.— As figure 1 for targets with both Y and J band data (the gap between the two bands is shown by the long horizontal lines).

on the position of the target. The extracted 1D spectra were corrected for telluric absorption using observations of the nearest $V \sim 8$ A0V Hipparcos star, for galactic extinction using the Cardelli et al. (1989) extinction law with $R_V = 3.1$, and airmass. The absolute flux calibration was obtained from 3 bright objects ($F_{098M} = 20.43, 21.26$, and 19.57) with known HST magnitudes which were also observed in the MOSFIRE masks simultaneously with the dropouts, calculating slit losses based on the HST images. Each night of observations was reduced separately combining only the final spectral products at the very end. The final calibrated spectra are shown in Figures 1 and 2 and are consistent with noise. The sensitivity is consistent with that estimated by the MOSFIRE Exposure Time Calculator.

The non-detections allow us to rule out the possibility that the sources in BoRG_1510+1115 are lower redshift contaminants where the HST continuum flux comes from emission lines like [O II] and [O III] or [O III] and H β (Atek et al. 2011). However, if the continuum magnitude in F125W were due to an emission line, it would correspond to $\sim 2 - 8 \cdot 10^{-17}$ erg $s^{-1} \text{cm}^{-2}$, detectable with our median sensitivity of 0.4-0.6 in the same units ($5\text{-}\sigma$). Similarly, our sensitivity is sufficient to exclude contamination by red galaxies where a weaker line in J enhances the break as suggested by Capak et al. (2011). The exception would be for the fields with only Y coverage if weak [O III] fell beyond $1.1238 \mu\text{m}$ ($z > 1.244$) but within the F125W filter, while H α accounted for the flux in F160W.

Longer wavelength coverage with MOSFIRE is needed to rule out this possibility.

3. INFERENCES ON THE LY- α OPTICAL DEPTH

3.1. Summary of the method

We apply the method introduced by Treu et al. (2012) to constrain the distribution of equivalent width of Ly- α given a sample of LBGs, exploiting all the information available. Only a brief summary of the method is given here. The reader is referred to Treu et al. (2012) for details and analytic expressions of the likelihood.

As in our previous work we describe the intrinsic rest-frame distribution in terms of the one measured at $z \sim 6$ by Stark et al. (2011) $p_6(W)$

$$p_6(W) = \frac{2A}{\sqrt{2\pi}W_c} e^{-\frac{1}{2}\left(\frac{W}{W_c}\right)^2} H(W) + (1-A)\delta(W), \quad (1)$$

with $W_c=47\text{\AA}$, $A=0.38$ for sources with $-21.75 < M_{UV} < -20.25$ and $W_c=47\text{\AA}$, $A=0.89$ for sources with $-20.25 < M_{UV} < -18.75$. A is the fraction of emitters and H is the step function. As discussed below, $1-A$ includes the fraction of interlopers. Following Treu et al. (2012) we consider two extreme cases which should bracket the range of possible scenarios. In the first (“patchy”) model, no Ly α is received from a fraction ϵ_p of the sources, while the rest is unaffected. The probability distribution of the equivalent width is then given by

$$p_p(W) = \epsilon_p p_6(W) + (1 - \epsilon_p)\delta(W) = \frac{2A\epsilon_p}{\sqrt{2\pi}W_c} e^{-\frac{1}{2}\left(\frac{W}{W_c}\right)^2} H(W) + (1 - A\epsilon_p)\delta(W). \quad (2)$$

In the second (“smooth”) model, Ly α is attenuated by a factor ϵ_s , yielding

$$p_s(W) = p_6(W/\epsilon_s)/\epsilon_s = \frac{2A}{\sqrt{2\pi\epsilon_s}W_c} e^{-\frac{1}{2}\left(\frac{W}{\epsilon_s W_c}\right)^2} H(W) + (1 - A)\delta(W). \quad (3)$$

Bayes’s rule gives the posterior probability of ϵ_p and ϵ_s (collectively ϵ) and z given an observed spectrum and continuum magnitude m :

$$p(\epsilon, z_i | \{f\}, m) \propto \left[\prod_j \int dW p(f_j, m | W, z_i) p(W | \epsilon) \right] p(\epsilon) p(z_i), \quad (4)$$

where the term within square brackets is the likelihood $p(\{f\} | \epsilon, z_i, m)$, $f_j \in \{f\}$ are the flux measurements in each spectral pixel and $z_i = \lambda_i/\lambda_0 - 1$. We adopt a uniform prior $p(\epsilon)$ between zero and unity, while the prior $p(z_i)$ is given by the photometric redshift. By construction our method takes into account the strong wavelength dependence of the sensitivity typical of near infrared spectroscopic data. The inference is carried out for each spectral pixel, using its noise properties including the effects of atmospheric transmission and absorption.

The posterior on ϵ is obtained by summing over z_i in the range where $p(z_i)$ is non-zero. Our formalism takes properly into account the effects of incomplete wavelength coverage, in deriving limits on ϵ and z_i . For example, if the wavelength range only covers an interval $[z_{\min}, z_{\max}]$, and the prior on ϵ is uniform, then the posterior will be:

$$p(\epsilon | \{f\}, m) \propto \sum_{z_i \in [z_{\min}, z_{\max}]} p(\{f\} | \epsilon, z_i, m) p(z_i) + p(\{f\} | \epsilon = 0) p(z_i \notin [z_{\min}, z_{\max}]) \quad (5)$$

The normalization factor Z is the Bayesian evidence and quantifies how well the model describes the data. It can be used for selection, by comparing evidence ratio between two models, or to decide whether additional parameters are warranted by the data. In comparison to other standard model selection techniques like likelihood ratio the advantage of the evidence is that it takes into account the entire parameter space, thus avoiding issues of fine tuning.

The formalism described above is for an individual galaxies. For a sample of galaxies, or for multiple independent spectra of the same galaxies, it is sufficient to multiply the likelihoods to obtain the total likelihood.

3.2. Results

The key result of this paper is the posterior probability densities of the ϵ_p and ϵ_s parameters given the data, shown in Figure 3. This posterior probability distribution function is based on the 8-non detections of the primary sample presented here, plus the three non-detections presented by Treu et al. (2012) and Schenker et al. (2012)². The non-detections imply that Ly α emission is suppressed significantly between $z \sim 6$ and $z \sim 8$. The 68% credible intervals, obtained by integrating the posterior are $\epsilon_p < 0.31$ and $\epsilon_s < 0.28$, i.e. Ly α emission from LBGs is less than a third than the value at $z \sim 6$. The parameters ϵ_p and ϵ_s can be physically interpreted as the average excess optical depth of Ly- α with respect to $z \sim 6$, i.e. $\langle e^{-\tau_{Ly\alpha}} \rangle$. As expected for a sample of non-detections, the data are insufficient to distinguish between the two models. We will thus refer primarily to the patchy model, for easier comparison with previous work (this is the model implicitly assumed by Fontana et al. 2010; Pentericci et al. 2011; Ono et al. 2012; Schenker et al. 2012).

Before discussing the interpretation of our findings we need to consider the role of contamination. The parameter ϵ_p relates the number of LBG selected galaxies with Ly α emission at $z \sim 8$ to the same quantity at $z \sim 6$. In order to transform this into a Ly α optical depth, one has to account for the fraction of contaminants in both samples

$$n_{Ly\alpha, z=8} = \epsilon_p n_{Ly\alpha, z=6} \frac{1 - f_6}{1 - f_8}, \quad (6)$$

where f_6 and f_8 are the fraction of contaminants in the $z \sim 6$ and $z \sim 8$ LBG selected samples, respectively. A simple estimate of the number of contaminants can be obtained from the posterior probability distribution functions of the photometric redshifts and by computing the total probabilities that the source is outside the fiducial window. This probability is low and does not change our conclusions in any significant way: Stark et al. (2011) estimate $f_6 < 0.1$ with this method, while for our method it is in the range 0.1-0.2 and already taken into account by our formalism as described by Treu et al. (2012). A more insidious form of contaminants is represented by the

² BORG11534, A1703_zD7 and BORG58, The latter is also part of the MOSFIRE sample presented here, so the total number of objects is 10, with one having two independent observations with different wavelength coverage and sensitivity.

TABLE 1
SUMMARY OF HIGH REDSHIFT CANDIDATES OBSERVED WITH MOSFIRE

Object	α_{J2000}	δ_{J2000}	V_{606}	Y_{098}	J_{125}	H_{160}	Stat.	t_{exp}/hr	$\sigma_W/\text{\AA}$
0951+3304_0180	147.70451	33.06513	>26.83	>26.83	26.24 ± 0.27	26.56 ± 0.43	1	1	4.1
0951+3304_0277	147.68443	33.07019	>26.83	>26.83	25.87 ± 0.22	25.88 ± 0.27	1	1	3.0
1437+5043_r2_0637_T12a	219.21058	50.72601	>28.10	>28.05	25.76 ± 0.07	25.69 ± 0.08	1	3	2.1
1510+1115_0354	227.54706	11.23145	>27.59	>27.83	27.03 ± 0.22	27.21 ± 0.38	1	2.1, 3	9.3
1510+1115_1218	227.54266	11.26152	>27.59	>27.83	26.87 ± 0.22	26.64 ± 0.25	1	2.1, 3	8.6
1510+1115_1487	227.53173	11.25254	>27.59	>27.83	27.60 ± 0.24	27.34 ± 0.28	1	2.1, 3	15.7
1510+1115_1524	227.53812	11.25552	>27.59	>27.83	26.63 ± 0.15	26.52 ± 0.20	1	2.1, 3	6.6
1510+1115_1705	227.54008	11.25111	>27.59	>27.83	27.00 ± 0.19	27.02 ± 0.28	1	2.1, 3	9.2
<hr/>									
1437+5043_r2_0070_T12e	219.22225	50.70808	>28.10	>28.05	26.90 ± 0.14	26.94 ± 0.17	0	3	6.0
1437+5043_r2_0388	219.23494	50.71960	>28.10	>28.05	27.66 ± 0.24	27.84 ± 0.36	0	3	11.5
1437+5043_r2_0560_T12c	219.23092	50.72405	27.92 ± 0.31	>28.05	27.73 ± 0.23	27.47 ± 0.24	0	3	12.4
1437+5043_r3_0279	219.18681	50.72723	>27.94	>27.82	27.27 ± 0.24	27.46 ± 0.34	0	3	8.4
1437+5043_r3_0447	219.18983	50.73406	>27.94	>27.82	27.63 ± 0.27	>27.79	0	3	12.3

NOTE. — Photometry is taken from the most recent analysis by Schmidt et al. (2013; in preparation). and has been corrected for Galactic extinction using the Cardelli et al. (1989) extinction law and E(B-V) of 0.01328, 0.01254, and 0.04605 for BoRG_0951+3304, BoRG_1437+5043 and BoRG_1510+1115 respectively. The candidates in the field 1437+5043 were identified by Trenti et al. (2012) and Bradley et al. (2012). The magnitude limits are 2σ limits. The candidates in the first part of the table (Stat=1) satisfy all the requirements for Y-dropout selection and are the statistical sample analyzed in this paper. The candidates below the horizontal bar (Stat=0) were observed as slit fillers. The t_{exp}/hr give the total exposure time in Y(, J). The last column lists the median Ly α equivalent width noise (1σ) of the MOSFIRE spectra.

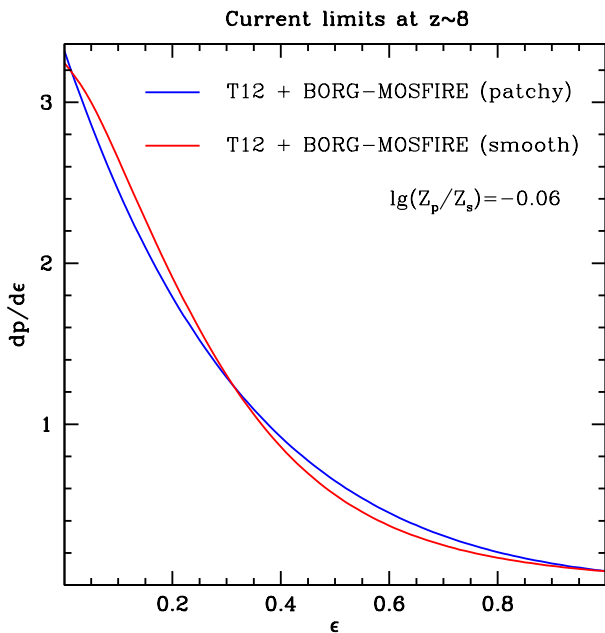


FIG. 3.— Inference results in the context of the patchy and smooth models described in the text. The parameter ϵ describes the change of the Ly α equivalent width distribution between $z \sim 6$ and $z \sim 8$. In the patchy model, at any given equivalent width, only a fraction ϵ_p of the sources that are emitting at $z \sim 6$ are found to be emitters at $z \sim 8$. In the smooth model the emission of each source is suppressed by a factor ϵ_s . The evidence ratio Z_p/Z_s is inconclusive and does not favor any of the two models. The results shown are based on the 8 objects in the primary MOSFIRE sample presented here as well as the three spectra analyzed by Treu et al. (2012).

“unknown unknowns”, like the faint emission line objects discussed above.

In the case of BoRG this additional contribution is estimated to be $f_8 \sim 0.2$, (bringing the total to 0.33-0.42 Bradley et al. 2012). In the case of the i-dropouts selected from GOODS (Stark et al. 2011), the additional contamination is probably somewhat less, given the higher quality of the dithering strategy and larger number of blue bands available.

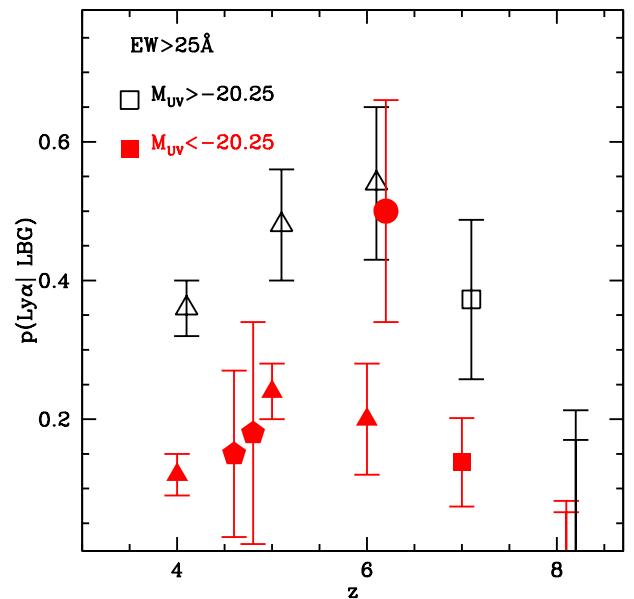


FIG. 4.— Evolution of the fraction of LBGs with Ly- $\alpha > 25 \text{ \AA}$ equivalent width (rest frame), for bright (filled red symbols) and faint galaxies (open black symbols). Triangles are taken from Stark et al. (2011) and Schenker et al. (2012), pentagons from Mallery et al. (2012) and the circle is from Curtis-Lake et al. (2012). The squares at $z \sim 7$ are taken from Treu et al. (2012) and are based on a compilation of data (Fontana et al. 2010; Vanzella et al. 2011; Pentericci et al. 2011; Ono et al. 2012; Schenker et al. 2012). The upper limits at $z \sim 8$ are from this paper. The lower and higher horizontal bars on the upper limits at $z \sim 8$ describe the range of uncertainty stemming from contaminants in the photometrically selected LBG sample.

To be conservative we thus consider the ratio $(1-f_6)/(1-f_8)$ to be in the range 1-1.25, that is from equal contamination – after accounting for known losses inferred from photo-zs – to higher contamination in the $z \sim 8$ sample.

With this estimate in hand we can proceed to compute the fraction of LBGs with Ly α emission above the standard

threshold of 25\AA equivalent width. Our measurement at $z \sim 8$ is shown in Figure 4 together with data from the literature at lower redshift (see caption). In the patchy model, the fractions for Y-dropouts are $< 0.07 - 0.08$ for galaxies with $M_{UV} < -20.25$ and $< 0.17 - 0.21$ for galaxies fainter than this limit (the two numbers are for minimal and maximal contamination). In the smooth model the same fractions are $< 0.03 - 0.05$ and $0.06 - 0.12$. Note that these bounds include the uncertainty on the $z \sim 6$ fraction and thus the uncertainties on the points beyond $z \sim 6$ are correlated. If the fractions at $z \sim 6$ move up/down, so do the points at higher redshift, but the trend will remain the same. Even considering the more conservative upper limits from the patchy model, the drop in the fraction of Ly α emitters amongst LBG in just 300 Myrs is at least a factor of ~ 3 .

There are three possible explanations for our finding, ranging from the mundane to the very interesting. The first and most mundane explanation is that samples of Y-dropouts suffer from much higher rate of contamination than similar LBG samples at lower redshift. A breakdown of the Lyman Break technique could occur if there were exotic populations of galaxies which are missing from our current templates and models used to estimate color-cuts and compute photo-zs. While this cannot be ruled out with present data, it would certainly be a surprise to see the Lyman Break selection breaking down so abruptly over a relatively small change in wavelength and magnitudes. The second explanation could be related to the special environment of the BoRG galaxies. As expected for the most luminous galaxies at every redshift, the BoRG sources are bright and strongly clustered, especially those that we selected for spectroscopic follow-up (Hildebrandt et al. 2009; Overzier et al. 2009). Thus, we may be comparing galaxies in proto-clusters with field galaxies, and perhaps this could bias our interpretation. However, we expect the higher density regions to completely reionize earlier and therefore to have a smaller Ly α optical depth, not larger (Barkana & Loeb 2004). Thus this second explanation of the large Ly α optical depth at $z \sim 8$ as the result of a selection bias would also be surprising. The third explanation is that indeed the average Ly α optical depth of the universe increases significantly in this small amount of cosmic time. This third explanation would be very exciting, implying that we have reached an epoch where the properties of the intergalactic and circumgalactic medium (IGM and CGM, respectively) are changing dramatically, presumably owing to rapid changes in the degree of cosmic reionization or in the physics of the first generations of star forming regions.

Observationally, the big question is then how do we test these three hypothesis. Searches for Ly α to greater depth than ours, would provide useful information, hopefully including detections. But also more and deeper non-detections would certainly help tighten the upper limits derived here. This is possible with longer MOSFIRE integrations or by using the WFC3 grism on board the Hubble Space Telescope. Systematic studies of many gravitationally lensed sources should be a particularly powerful way to probe very faint sources and thus also help with testing the second hypothesis (e.g., Bradač et al. 2012). However, it is probable that some fraction of LBGs at $z \sim 8$ and above will remain undetected in Ly α even with heroic efforts. In order to quantify the amount of contaminants and thus test the first and third hy-

potheses, one needs detections of other lines or of the continuum. Hopefully IR lines can be detected with pointed observations with ALMA (Carilli & Walter 2013) although this is non-trivial (Ouchi et al. 2013). Detection of the continuum will be hard and might require several hours of integrations with the James Webb Space Telescope (Treu et al. 2012) or an extremely large telescope like the Thirty Meter Telescope, unless the sources are highly magnified by a foreground gravitational lens.

4. CONCLUSIONS

We present MOSFIRE observations of a sample of candidate $z \sim 8$ galaxies identified as part of the BoRG Survey. The data are consistent with noise, setting stringent upper limits on the presence of emission lines. We carry out a statistical analysis of the non-detections in the context of our flexible models of purely patchy and smooth absorption showing that they imply a substantial increase in Ly α optical depth $\tau_{Ly\alpha}$ between $z \sim 6$ and $z \sim 8$. Quantitatively, our findings can be summarized as follows:

- At $z \sim 8$ the distribution of Ly- α equivalent width is significantly reduced with respect to $z \sim 6$, by at least a factor of three (i.e. $\langle e^{-\tau_{Ly\alpha}} \rangle < 0.31$ and < 0.28 respectively in the patchy and smooth model).
- The fraction of emitters with equivalent width $> 25\text{\AA}$ can be computed within our models. In the patchy model, the fractions for Y-dropouts are $< 0.06 - 0.08$ for galaxies with $M_{UV} < -20.25$ and $< 0.16 - 0.21$ for galaxies fainter than this limit (the two numbers are for minimal and maximal contamination). In the smooth model the same fractions are $< 0.03 - 0.05$ and $0.06 - 0.12$.

These results extend out to $z \sim 8$ in a more dramatic fashion the increase in Ly α optical depth seen by previous studies between $z \sim 6$ and $z \sim 7$ (Fontana et al. 2010; Vanzella et al. 2011; Pentericci et al. 2011; Schenker et al. 2012; Ono et al. 2012; Treu et al. 2012). This body of work indicates that the properties of LBG galaxies are evolving over a very short amount of cosmic time. More spectroscopic data are needed to characterize this very interesting process further and clarify the relationship between the vanishing Ly α emission and cosmic reionization.

Some of the data presented herein were obtained at the W.M. Keck Observatory. The authors wish to recognize and acknowledge the very significant cultural role and reverence that the summit of Mauna Kea has always had within the indigenous Hawaiian community. We are grateful to the MOSFIRE team and the staff at Keck for making these observations possible, and to N.P.Konidaris for writing the data reduction pipeline. This paper is also based on observations made with the NASA/ESA Hubble Space Telescope, obtained at the Space Telescope Science Institute. We acknowledge support through grants HST-11700, 12572, 12905, and we thank the referee for a constructive report, which improved the manuscript. T.T. thanks L.Pentericci, E.Vanzella, M.Giavalisco, and D.Stark for useful conversations.

REFERENCES

- Bouwens, R. J., Illingworth, G. D., Oesch, P. A., et al. 2010, *ApJ*, 709, L133
- Bradač, M., Vanzella, E., Hall, N., et al. 2012, *ApJ*, 755, L7
- Bradley, L. D., Trenti, M., Oesch, P. A., et al. 2012, *ApJ*, 760, 108
- Bunker, A. J., Caruana, J., Wilkins, S. M., et al. 2013, *MNRAS*, 430, 3314
- Capak, P., Mobasher, B., Scoville, N. Z., et al. 2011, *ApJ*, 730, 68
- Capak, P., Faisst, A., Vieira, J. D., et al. 2013, *ApJ*, 773, L14
- Cardelli, J. A., Clayton, G. C., & Mathis, J. S. 1989, *ApJ*, 345, 245
- Carilli, C., & Walter, F. 2013, arXiv:1301.0371
- Coe, D., Zitrin, A., Carrasco, M., et al. 2013, *ApJ*, 762, 32
- Curtis-Lake, E., McLure, R. J., Pearce, H. J., et al. 2012, *MNRAS*, 422, 1425
- Ellis, R. S., McLure, R. J., Dunlop, J. S., et al. 2013, *ApJ*, 763, L7
- Fontana, A., Vanzella, E., Pentericci, L., et al. 2010, *ApJ*, 725, L205
- Hildebrandt, H., Pielorz, J., Erben, T., et al. 2009, *A&A*, 498, 725
- Jiang, L., Bian, F., Fan, X., et al. 2013, *ApJ*, 771, L6
- Kashikawa, N., Shimasaku, K., Malkan, M. A., et al. 2006, *ApJ*, 648, 7
- Lehnert, M. D., Nesvadba, N. P. H., Cuby, J.-G., et al. 2010, *Nature*, 467, 940
- Lorenzoni, S., Bunker, A. J., Wilkins, S. M., et al. 2011, *MNRAS*, 414, 1455
- Mallery, R. P., Mobasher, B., Capak, P., et al. 2012, *ApJ*, 760, 128
- McLean, I. S., Steidel, C. C., Matthews, K., Epps, H., & Adkins, S. M. 2008, *Proc. SPIE*, 7014,
- McLean, I. S., Steidel, C. C., Epps, H. W., et al. 2012, *Ground-based and Airborne Instrumentation for Astronomy IV. Proceedings of the SPIE*, 8446, doi:10.1117/12.924794
- Oesch, P. A., Bouwens, R. J., Illingworth, G. D., et al. 2013, *ArXiv e-prints*, arXiv:1301.6162
- Ono, Y., Ouchi, M., Mobasher, B., et al. 2012, *ApJ*, 744, 83
- Ouchi, M., Ellis, R., Ono, Y., et al. 2013, *ArXiv e-prints*, arXiv:1306.3572
- Overzier, R. A., Guo, Q., Kauffmann, G., et al. 2009, *MNRAS*, 394, 577
- Pentericci, L., Fontana, A., Vanzella, E., et al. 2011, *ApJ*, 743, 132
- Robertson, B. E., Furlanetto, S. R., Schneider, E., et al. 2013, *ApJ*, 768, 71
- Schenker, M. A., Stark, D. P., Ellis, R. S., et al. 2012, *ApJ*, 744, 179
- Stark, D. P., Ellis, R. S., & Ouchi, M. 2011, *ApJ*, 728, L2+
- Trenti, M., Stiavelli, M., Bouwens, R. J., et al. 2010, *ApJ*, 714, L202
- Trenti, M., Bradley, L. D., Stiavelli, M., et al. 2011, *ApJ*, 727, L39+
- Trenti, M., Bradley, L. D., Stiavelli, M., et al. 2012, *The Astrophysical Journal*, 746, 55
- Treu, T., Trenti, M., Stiavelli, M., Auger, M. W., & Bradley, L. D. 2012, *ApJ*, 747, 27
- Vanzella, E., Pentericci, L., Fontana, A., et al. 2011, *ApJ*, 730, L35+